

Forward neutron production in fragmentation of high-energy heavy nuclei

Vladimir Yurevich¹

Joint Institute for Nuclear Research

Joliot Curie 6, Dubna, Moscow region, Russia

E-mail: yurevich@jinr.ru

Production of quasi-monoenergetic beam of GeV neutrons by fragmentation of high-energy heavy nuclei in nuclear interactions in a target is discussed. It is shown that picosecond pulses of GeV neutrons with energy spread $< 4\%$ can be realized with available beams of Pb and Au ions at SPS/CERN and AGS/BNL.

*54th International Winter Meeting on Nuclear Physics
25-29 January 2016
Bormio, Italy*

¹Speaker

© Copyright owned by the author(s) under the terms of the Creative Commons Attribution-NonCommercial-NoDerivatives 4.0 International License (CC BY-NC-ND 4.0).

<http://pos.sissa.it/>

1. Introduction

The relativistic beams of Pb ions at SPS/CERN and Au ions at AGS/BNL give a unique opportunity to produce a beam of quasi-monoenergetic neutrons with energy above 10 GeV by fragmentation of heavy ions in collisions with targets of light-mass nuclei. This is a very promising method to study of neutron – proton and neutron – nucleus collisions in GeV energy range.

At the present time, however, it is rather difficult to reproduce distributions of these neutrons using theoretical models and codes requiring further development and verification. A phenomenological analysis of available experimental data on neutron production in nuclear reactions at high energies is an alternative approach. In this study, characteristics of the emitted relativistic neutrons are calculated using the Lorentz transformation of neutron distributions obtained in a Moving Source Model analysis of experimental data on neutron production in $p + \text{Pb}$ and $\text{C} + \text{Pb}$ reactions at GeV energies [1-4]. The results are applied for estimation of parameters of neutron beam produced in interaction of Pb-ion beam with light-mass nuclei of a target.

2. Neutron production in high-energy reactions with heavy nuclei

The decay of a nuclear system produced in collisions of relativistic hadrons and light-mass nuclei with heavy nuclei is a complicated process and it consists of different stages of the nuclear system evolution. The analysis of experimental data on emission of charged particles, fragments, and neutrons in high-energy reactions supports this picture of the nuclear system evolution and decay with four main stages-sources. This approach was realized in a Moving Source Model (MSM) with four neutron sources: S_1 – cascade stage, S_2 – hot source decay, S_3 – multifragmentation, and S_4 – evaporation [1-4]. The second and third sources occur only in central collisions. The MSM expression is based on an assumption about thermal equilibrium in each particle sources and isotropic emission in the source frame. The formula has four terms in correspondence with the number of neutron sources

$$\frac{d^2\sigma}{dE_{kin}d\Omega} = \sum_{i=1}^4 pA_i \exp\left\{-\left(\frac{E_{kin} + m - p\beta_i \cos\theta}{(1 - \beta_i^2)^{1/2}} - m\right)/T_i\right\}, \quad (1)$$

where E_{kin} and θ are the kinetic energy (MeV) and the angle of the emitted neutron in the lab. frame respectively, p – the neutron momentum, Ω – the solid angle, T – the temperature parameter (MeV). There are three parameters for each source: the amplitude A_i , the temperature T_i and the normalized velocity $\beta_i = V_i/c$. For $p + \text{Pb}$ and $\text{C} + \text{Pb}$ reactions at energy of several GeV the source temperatures are $T_1 \approx 70$ MeV, $T_2 \approx 21$ MeV, $T_3 \approx 4.7$ MeV, $T_4 \approx 1.6$ MeV, and the source velocities were estimated as $\beta_1 \approx 0.2$, $\beta_2 \approx 0.03$, $\beta_3 \approx 0.005$, and $\beta_4 \approx 0$. Examples of fitting experimental data [3,4] with expression (1) are shown in Fig.1 where the contributions of different stages-sources are the dashed curves. The source contributions to the neutron yield for these reactions at 2-GeV/u beam energy are shown in Fig.2. For reactions with heavy nuclei the main contributions come from the last two stages, evaporation and multifragmentation.

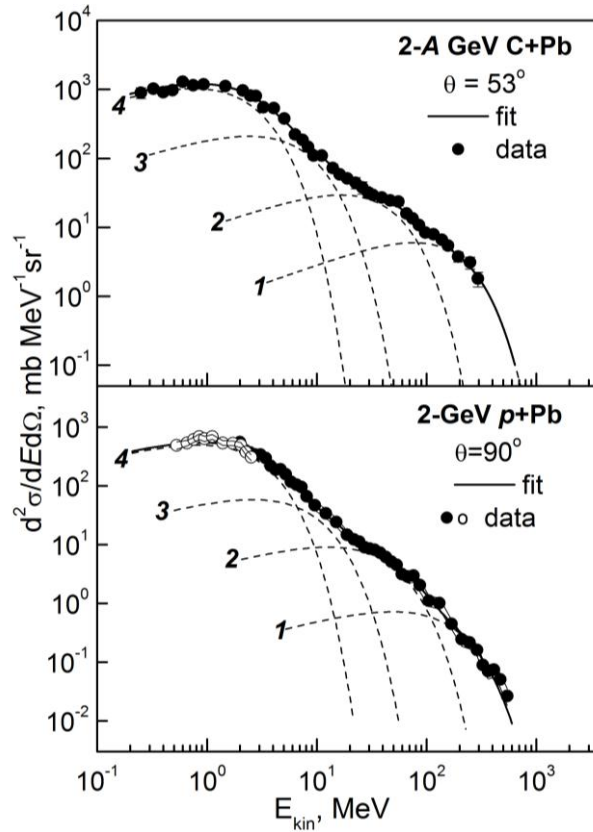


Fig.1. The source contributions to the neutron energy spectra for $p + \text{Pb}$ and $\text{C} + \text{Pb}$ reactions: the points – the experimental data [3,4], the curves – the contributions of different stages-sources.

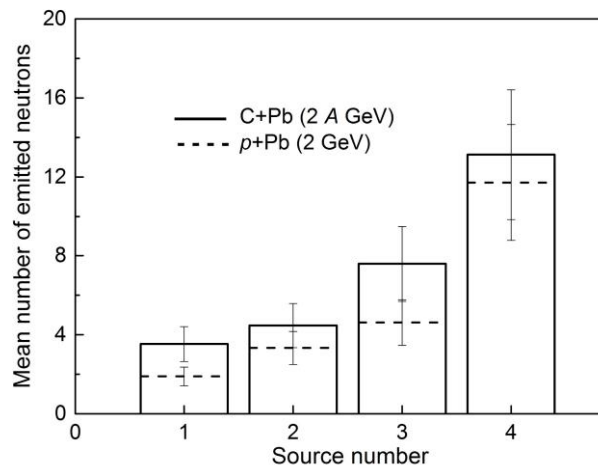


Fig.2. The source contributions to the neutron yield for $p + \text{Pb}$ and $\text{C} + \text{Pb}$ reactions at 2 GeV/u.

The energy deposition in ALICE neutron ZDC was recently measured for $p + \text{Pb}$ collisions at extremely high energy $\sqrt{s_{NN}} = 5.02 \text{ TeV}$ [5,6]. It corresponds to neutron multiplicity distribution with mean value $\langle M_n \rangle = 33.3$ neutrons shown in Fig.3. The mean neutron multiplicity as a function of the proton energy is shown in Fig.4 and it is well described by a formula

$$\langle M_n \rangle = 35 \left(1 - \frac{1.32}{E_{kin} + 1.4} \right). \quad (2)$$

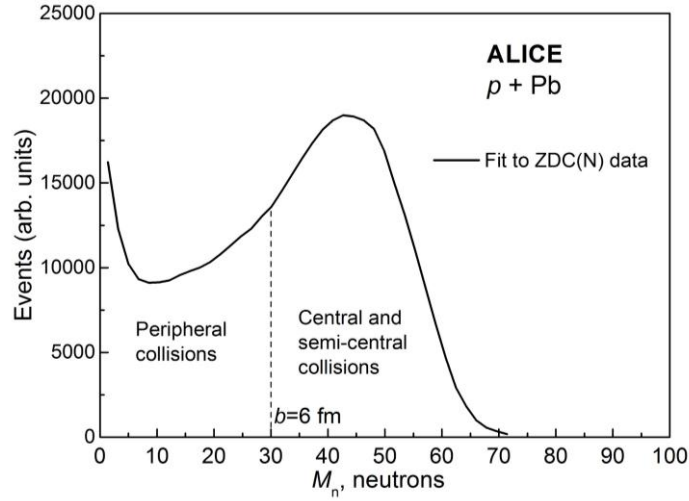


Fig.3. The neutron multiplicity distribution measured with ALICE neutron ZDC for $p + Pb$ collisions at $\sqrt{s_{NN}} = 5.02$ TeV.

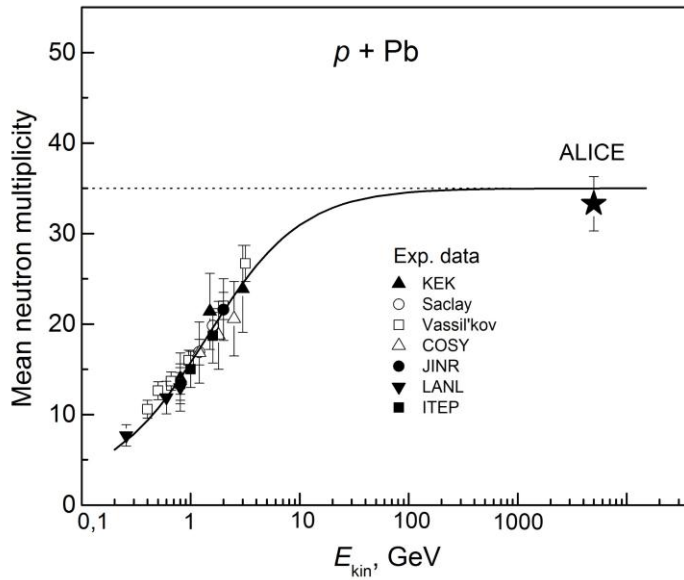


Fig.4. The mean neutron multiplicity as a function of the proton energy for $p + Pb$ collisions.

Above 10 GeV the mean neutron multiplicity saturates with energy with a limit value of 35 neutrons. But for individual min. bias events the neutron multiplicity changes from several to about 70 neutrons.

3. Neutron distributions in fragmentation of relativistic heavy nuclei

Estimation of characteristics of high-energy neutrons produced in fragmentation of relativistic Pb ions in interactions with light-mass nuclei of a target is reached by the Lorentz transformation of neutron distributions obtained by the MSM fitting experimental data for $p + \text{Pb}$ and $\text{C} + \text{Pb}$ reactions discussed above. In the inverse kinematics the neutron distributions dramatically change as it is shown in Fig.5 for $\text{Pb} + \text{C}$ and $\text{Pb} + \text{H}$ collisions.

The neutron distributions slightly depend on a type of target nuclei. The maximum intensity of neutrons is observed at angle $\theta = 0^\circ$ and the intensity rapidly drops with the angle. At small angles the neutron spectra have a peak shape and position of the maximum is equal to the kinetic energy per nucleon of the Pb ions. The peak at 0° has Gaussian shape as it is shown in Fig.6.

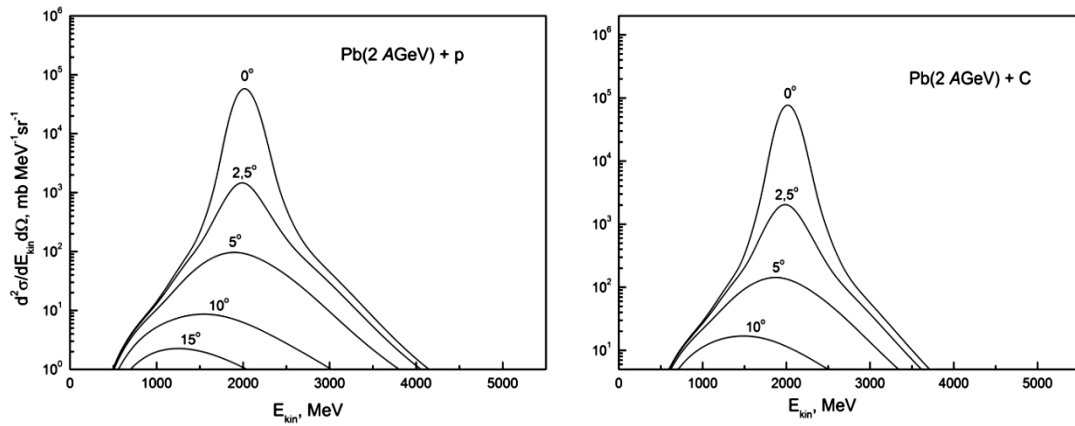


Fig.5. The energy spectra of neutrons at different angles for $\text{Pb} + \text{C}$ and $\text{Pb} + \text{H}$ collisions at energy of 2 GeV/u.

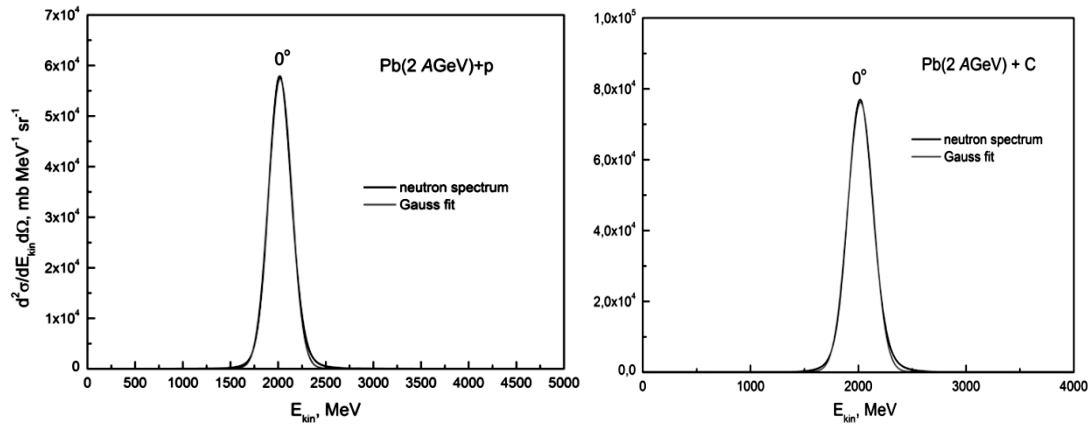


Fig.6. Neutron spectra at 0° with Gaussian fits for $\text{Pb} + \text{C}$ and $\text{Pb} + \text{H}$ collisions at energy of 2 GeV/u.

The relative energy spread decreases with the beam energy, or energy of neutrons. This dependence is shown in Fig.7 and it is clearly seen that the neutron energy distribution becomes similar to monoenergetic with small energy dispersion $\sigma_E/E_{kin} \leq 4\%$ above 6 GeV.

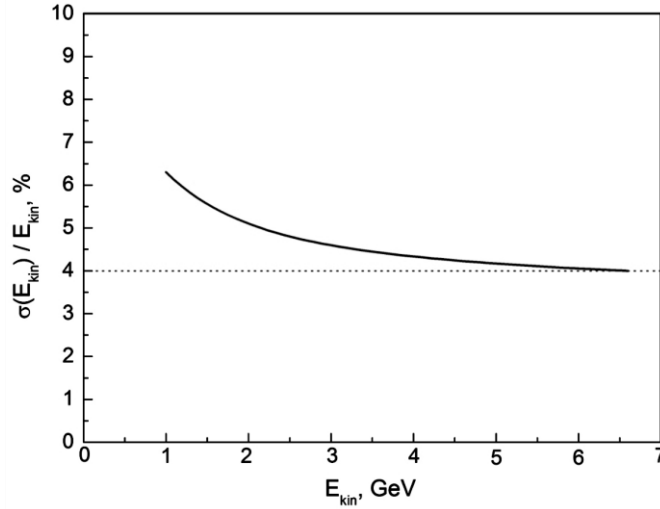


Fig.7. The energy resolution of neutron beam produced in fragmentation of Pb ions at $\theta = 0^\circ$ as a function of the kinetic energy.

4. Beam of quasi-monoenergetic relativistic neutrons

The beam of quasi-monoenergetic relativistic neutrons can be realized with available beams of 11-GeV/u Au ions at AGS/BNL and 20 – 158 – GeV/u Pb ions at SPS/CERN. At the maximum energy of SPS and a distance of 100 m from a neutron production target about 75% of emitted neutrons come into a spot with radius of 8.6 cm. A possible scheme of the neutron beam line is presented in Fig.8.

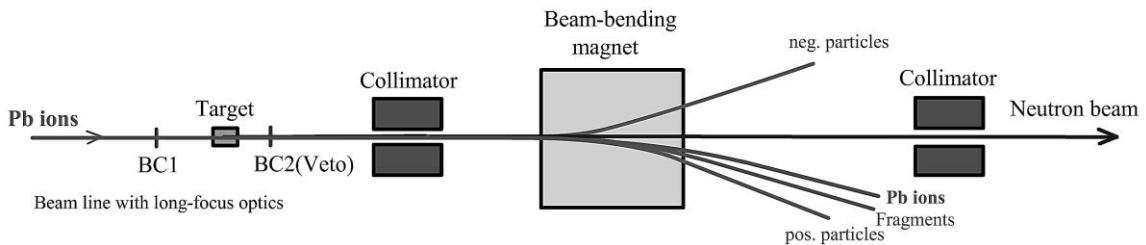


Fig.8. A scheme of the neutron beam line.

The main elements are a neutron production target, trigger detectors BC1 and BC2, collimators, and a beam-bending magnet. Each nuclear interaction in the target gives micropulse of neutrons produced simultaneously in the same reaction. A simple system of two beam

Cherenkov detectors BC1 and BC2 can be used for effective triggering the neutron pulses – the first detector registers incoming Pb ion in front of the target and the second one does not see the Pb ion behind the target. Application of MCP-PMTs in the detectors allows to reach the picosecond time resolution.

Let's consider an example of neutron beam produced in fragmentation of Pb ions of SPS beam with intensity $I_{\text{ion}} = 1 \times 10^6$ ion/s in 5% target (1.4-mm carbon or 1.9-mm polyethylene). Triggering central and semicentral collisions takes 60% of all nuclear interactions. The rate of neutron pulses is 3×10^4 pulses/s. The mean number of neutrons in beam spot per pulse is ≈ 34 neutron/pulse. Thus, the neutron beam intensity is $I_n \approx 1 \times 10^6$ neutron/s that is equal to the intensity of the ion beam. The neutrons in each pulse are coming approximately in the same time with a picosecond time spread.

5. Conclusion

Picosecond pulses of GeV neutrons at angle $\theta = 0^\circ$ with energy resolution $\sigma_E/E_{\text{kin}} < 4\%$ can be realized with available beams of Pb and Au ions at SPS/CERN and AGS/BNL. The interaction rate in the neutron production target defines the rate of neutron pulses. The achieved intensity of neutron beam is equal or exceeds the intensity of ion beam.

References

- [1] V. I. Yurevich, R. M. Yakovlev, V. G. Lyapin, *Physics of Atomic Nuclei* 69, 1469 (2006).
- [2] V. I. Yurevich, *Physics of Particles and Nuclei* 40, 49 (2009).
- [3] V. I. Yurevich, R. M. Yakovlev, V. G. Lyapin, *Physics of Atomic Nuclei* 74, 253 (2011).
- [4] V. I. Yurevich, R. M. Yakovlev, V. G. Lyapin, *Physics of Atomic Nuclei* 75, 192 (2012).
- [5] C. Oppedisano, *Nucl. Phys. A* 932, 399 (2014).
- [6] J. Adam et al., *Phys. Rev. C* 91, 064905 (2015).